TISSUE ENGINEERING: Part A
Volume 28, Numbers 21 and 22, 2022

DOI: 10.1089/ten.tea.2022.0054

termis
Tissue Engineering
& Regenerative Medicine
International Society

ORIGINAL ARTICLE

Human Lung Organoid Culture in Alginate With and Without Matrigel to Model Development and Disease

Briana R. Dye, PhD,[1] Joseph T. Decker, PhD,[1] Renee F.C. Hein, BS,[2] Alyssa J. Miller, PhD,[2] Sha Huang, BS,[2] Jason R. Spence, PhD,[2] and Lonnie D. Shea, PhD[1]

Human lung organoids (HLOs) are enabling the study of human lung development and disease by modeling native organ tissue structure, cellular composition, and cellular organization. In this report, we demonstrate that HLOs derived from human pluripotent stem cells cultured in alginate, a fully defined nonanimal product substrate, exhibit enhanced cellular differentiation compared with HLOs cultured in the commercially available Matrigel. More specifically, we observed an earlier onset and increase in the number of multiciliated cells, along with mucus producing $MUC5AC^+$ goblet-like cells that were not observed in HLOs cultured in Matrigel. The epithelium in alginate-grown HLOs was organized in a pseudostratified epithelium with airway basal cells lining the basal lamina, but with the apical surface of cells on the exterior of the organoid. We further observed that HLOs cultured in Matrigel exhibited mesenchymal overgrowth that was not present in alginate cultures. The containment of the mesenchyme within HLOs in alginate enabled modeling of key features of idiopathic pulmonary fibrosis (IPF) by treatment with transforming growth factor β (TGFβ). TGFβ treatment resulted in morphological changes including an increase in mesenchymal growth, increased expression of IPF markers, and decreased numbers of alveolar-like cells. This culture system provides a model to study the interaction of the mesenchyme with the epithelium during lung development and diseased states such as IPF.

Keywords: lung, organoids, alginate, hydrogels, stem cells

Impact Statement

Human lung organoids (HLOs) can potentially be used as model systems for diseases of the lung; however, they are currently limited by the ability of existing culture systems to support functional organoids. In this study, we describe an alginate culture system that supports the development of HLOs from embryonic stem cells. Organoids grown in alginate both model key aspects of lung physiology and display hallmarks of fibrosis when stimulated with transforming growth factor β. This model system could potentially be used to screen treatments for fibrotic lungs and provide crucial insights into lung biology.

Introduction

Breakthroughs in three-dimensional (3D) tissue models called organoids have provided new approaches to study human tissue development, homeostasis, and disease by modeling native organ tissue structure, cellular composition, and cellular organization.[1–5] Three-dimensional lung models, including our work with human lung organoids (HLOs), have provided models for the study of lung development, diseases such as idiopathic lung fibrosis or cystic

Departments of [1]Biomedical Engineering and [2]Internal Medicine, Gastroenterology, University of Michigan, Ann Arbor, Michigan, USA.

fibrosis, and infections.[6–10] The 3D environment of an organoid is hypothesized to be crucial to promote and sustain tissue structures that contain multiple cell types and resemble the native organ. These structures and cell types are necessary for modeling disease that may impact multiple cell types and tissues within an organ.

The majority of these complex model systems have been grown in a 3D droplet of Matrigel, which is a matrix derived from mouse sarcoma cells consisting of extracellular matrix (ECM) proteins and growth factors.[5] HLOs derived from human pluripotent stem cells (hPSCs) grown in Matrigel consist of an epithelium and mesenchyme, and after 65 days in culture, the HLOs have airway-like epithelial structures that contain $P63^+$ basal cells and few ciliated cells. In addition, HLOs contain scattered alveolar-like cells, which make up the gas exchanging units in the native lung.[7] This model provides a means to study epithelium and mesenchymal interactions and airway development and disorders. This HLO model resembles early fetal airway and only matures into a more adult-like airway when grown in an *in vivo* environment such as a mouse fat pad.[7]

Although Matrigel supports the growth of a wide range of organoid tissue models, this matrix is an undefined animal product that limits translational applications. Furthermore, Matrigel exhibits batch-to-batch variability. Finally, Matrigel causes mesenchyme outgrowth that is required to be trimmed away by scalpel every 2 weeks. A defined environment may restrict mesenchymal growth allowing for more controlled studies of epithelial and mesenchymal interactions and may lead to further maturation without the need of transplanting the organoid into an *in vivo* environment.

Combined, these limitations have motivated the development of alternative substrates for 3D tissue modeling systems, including synthetic hydrogels or alginate.[11–16] Multiple varieties of hydrogels have been developed that offer a ''tunable'' structure with controlled mechanical properties that can affect organoid cellular composition.[12,15,17] Alginate in particular is an inexpensive, accessible natural biomaterial derived from algae that forms a solid when crosslinked with calcium. Hydrogels from alginate have long been used for the *in vitro* culture of cells such as mesenchymal stem cells and chondrocytes[18–21] as well as tissues including primary ovarian follicles.[22,23] Recently, alginate has been shown to maintain cellular organization in human intestinal organoids compared with Matrigel-cultured intestinal organoids.[13]

In this report, we investigated alginate for the culture of HLOs. HLOs were derived from hPSCs and cultured in a stepwise manner following the native lung developmental events as previously described.[7,24] We analyzed the survival, morphology, and mesenchymal outgrowth of alginate-grown HLOs relative to cultures in Matrigel, as well as gene expression. The cellular organization and architectures of HLOs were also analyzed by histology for airway-like structures and cell types. The cultures were grown in the presence of transforming growth factor β (TGFβ), a factor associated with lung fibrosis, with similar analyses performed. Alginate-based culture system provides a supportive 3D environment for HLO growth and maturation, producing HLOs that form structures resembling the native lung, including functional multiciliated and mucous-producing airway-like cells. Furthermore, HLOs grown in alginate have both epithelial and mesenchymal cells and may serve as a model of idiopathic pulmonary fibrosis (IPF).

Materials and Methods

Maintenance of hPSCs and generation of HLOs

H1 human embryonic stem cell (hESC) line (NIH registry No. 0043) was obtained from the WiCell Research Institute and was used to derive all HLOs for these experiments. H1 hESCs were approved by the University of Michigan Human Pluripotent Stem Cell Research Oversight Committee. hESCs were maintained as previously described.[25] HLOs were derived as previously described[7] and placed in ratios of 100% Matrigel or 1–2% alginate (Cat. No. B25266; Alfa Aesar). Roughly 50 foregut spheroids were suspended in Matrigel or alginate and placed in a 50 μL droplet. The alginate was formed by placing a 5 μL 2% $CaCl_2$ droplet on the bottom of the well and then dropping the spheroids suspended in 45 μL of alginate (1–2%, with varying ratios of Matrigel). Healthy HLOs were defined as organoids that maintained their structure and size or increased in size.

Immunohistochemistry and imaging

Immunostaining was carried out as previously described.[26] Antibody information and dilutions are given in Table 1. All images and videos were taken on a Nikon A1 confocal microscope or a Zeiss Axio Observer.Z1. Imaris software was used to render Z-stack 3D images.

RNA extraction and quantitative reverse transcriptase polymerase chain reaction

RNA was extracted from organoids using a High Pure RNA Isolation Kit (Roche; Cat. No. 50-997-731). The biomaterial was physically removed from the HLO before RNA extraction, after which the HLO was washed in phosphate-buffered saline three times for ~5 min. RNA quantity and quality were determined spectrophotometrically, using a Nano Drop 2000 (Thermoscientific). Reverse transcription was conducted using the iScript(tm) Select cDNA Synthesis Kit (BioRad; Cat. No. BIO1708891) according to manufacturer's protocol. Finally, quantitative reverse transcriptase polymerase chain reaction (qRT-PCR) was carried out using Quantitect Sybr Green MasterMix (Qiagen; Cat. No. 204145) on a CFX Connect Real-Time PCR system (BioRad). For a list of primer sequences see Table 2. Data were normalized to gene expression in hPSCs.

Single-cell RNA sequencing

HLOs were digested to single cells as previously described[27] and sequenced on the 10×Chromium at the University of Michigan Sequencing Core. Raw sequencing data were processed using the Cell Ranger software package (10×Genomics) and was performed by the University of Michigan Advanced Genomics Core. The Seurat R package (version 3.1.5) was subsequently used to analyze the processed single-cell RNA sequencing (scRNAseq) data.[28] Cells with mitochondrial transcript counts >5%, along with cells with <300 and >2500 transcripts were discarded. Datasets were scaled and normalized before integration and clustering. Integration was performed using 2000 anchor genes, which

Table 1. Primary and Secondary Antibody Information

	Source	*Cat. No.*	*Dilution*	*Clone*
Primary antibody				
Biotin-mouse anti MUC5AC[a]	Abcam	ab79082	1:100	Monoclonal
Cy3- mouse anti-actin-α smooth muscle (SMA)[a]	Sigma	C6198	1:400	Monoclonal
Goat anti-β-catenin (βCAT)	Santa Cruz Biotechnology	sc-1496	1:200	C-18
Goat anti-P63	R&D	AF1916	1:500	Polyclonal
Goat anti-SOX9	R&D Systems	AF3075	1:500	Polyclonal
Mouse anti-acetylated tubulin (ACTTUB)	Sigma-Aldrich	T7451	1:1000	6-11B-1
Mouse anti-E-cadherin (ECAD)	BD Transduction Laboratories	610181	1:500	36/E-Cadherin
Rabbit anti-NKX2.1	Abcam	ab76013	1:200	EP1584Y
Rabbit anti-N-terminal pro SP-C (SFTPC)	Seven Hills Bioreagents	WRAB-9337	1:200	aa1-35
Secondary antibody				
Donkey anti-goat 647	Life Technologies	A-21447	1:500	
Donkey anti-goat Cy3	Jackson Immuno	705-165-147	1:500	
Donkey anti-mouse 488	Jackson Immuno	715-545-150	1:500	
Donkey anti-mouse Cy3	Jackson Immuno	715-165-150	1:500	
Donkey anti-rabbit 488	Jackson Immuno	711-545-152	1:500	
Donkey anti-rabbit Cy3	Jackson Immuno	711-165-102	1:500	
Streptavidin Dyligh 488	Thermo Fisher	PI21832	1:500	

[a]Secondary antibody conjugated to the primary antibody.

were subsequently used for dimensionality reduction through principal components analysis and Uniform Manifold Approximation and Projection. Clusters were identified using the ''FindCluster'' function. Differentially expressed genes for each cluster were identified using the ''FindConservedMarkers'' function and used to manually annotate cell type. Gene ontology was performed using Metascape.[29]

Organoid quantification

Healthy HLOs were quantified through the Zeiss Axio Vert.A1. Each gel droplet had ~3–7 HLOs. The percent of healthy HLOs per droplet was averaged and pulled together with the other droplets.

Experimental replicates and statistics

All experiments were carried out on at least three ($n=3$) independent biological samples per experiment. All error bars represent SEM, whereas the long bar represents the average. Statistical differences were assessed with Prism software using multiple *t*-tests.

Results

Alginate promotes HLO airway cell differentiation

We investigated the tissue morphology of HLOs cultured in 2% alginate crosslinked with 2% $CaCl_2$ in comparison with HLOs grown in a Matrigel droplet. In Matrigel, HLOs expanded and the mesenchyme grew from the body of the organoid (Fig. 1A). The mesenchyme outgrowth was removed every 2 weeks by trimming the mesenchyme around individual HLOs with a scalpel and placing them into a new Matrigel droplet. HLOs grown in 2% alginate had a strikingly different morphology relative to those in Matrigel. In alginate, the mesenchyme outgrowth was restrained and thus the organoids did not have to be manipulated throughout the

Table 2. qPCR Primers

Primer name	*Forward sequence*	*Reverse sequence*
COL1A1	AAGAGGAAGGCCAAGTCGAG	CACACGTCTCGGTCATGGTA
COL3A1	AGGGGAGCTGGCTACTTCTC	AGGACTGACCAAGATGGGAA
FOXJ1	CAACTTCTGCTACTTCCGCC	CGAGGCACTTTGATGAAGC
HOPX	GCCTTTCCGAGGAGGAGAC	TCTGTGACGGATCTGCACTC
MUC5AC[a]	GCACCAACGACAGGAAGGATGAG	CACGTTCCAGAGCCGGACAT
NKX2.1	CTCATGTTCATGCCGCTC	GACACCATGAGGAACAGCG
P63	CCACAGTACACGAACCTGGG	CCGTTCTGAATCTGCTGGTCC
PDX1	CGTCCGCTTGTTCTCCTC	CCTTTCCCATGGATGAAGTC
SCGB1A1	ATGAAACTCGCTGTCACCCT	GTTTCGATGACACGCTGAAA
SFTPC	AGCAAAGAGGTCCTGATGGA	CGATAAGAAGGCGTTTCAGG
SMA	CCAGAGCCATTGTCACACAC	CAGCCAAGCACTGTCAGG
T1alpha	ACATCCTTTGTTTTTGCCCA	AGTGTCATCTTCTGGCTGGC
Vimentin	CTTCAGAGAGAGGAAGCCGA	ATTCCACTTTGCGTTCAAGG

All above primer sequences were obtained from http://primerdepot.nci.nih.gov/ and all annealing temperatures 55°C unless stated otherwise.

[a]Annealing temperature 60°C.[44]

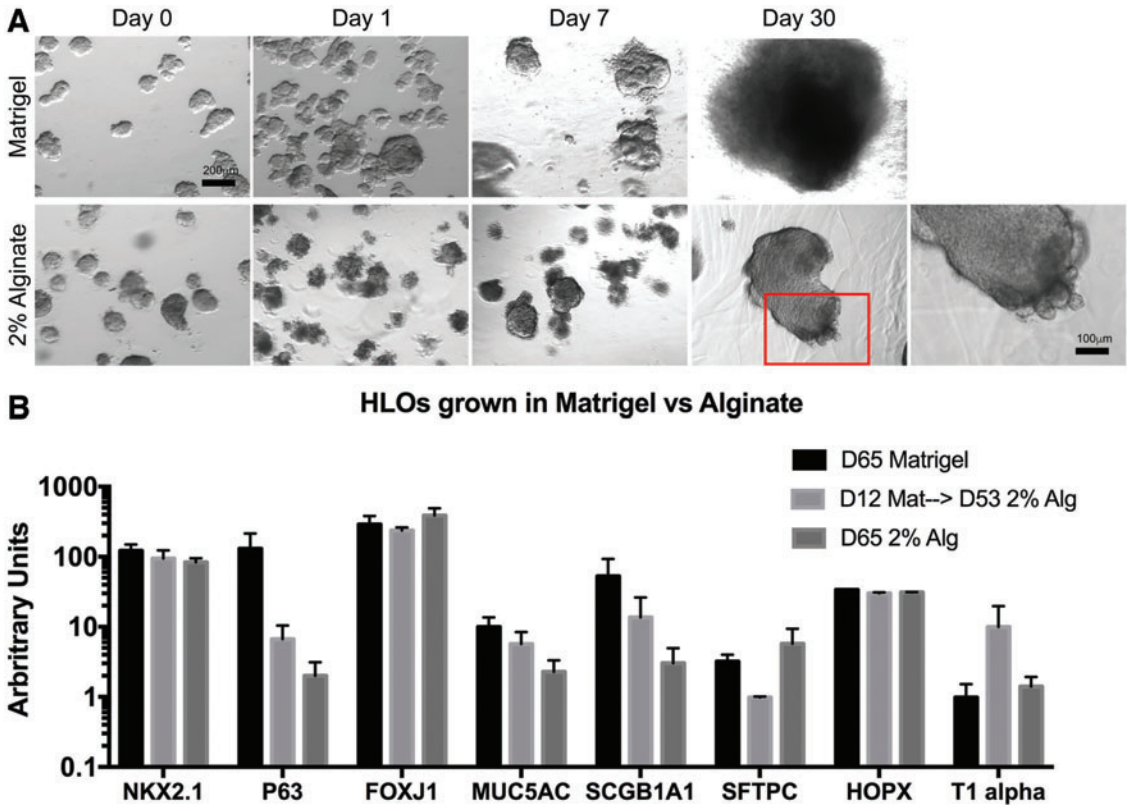

FIG. 1. HLOs grown in alginate form epithelial structures. **(A, B)** Wholemount images of HLOs grown in Matrigel **(A)** and 2% alginate. **(B)** Organoids cultured in Matrigel for 65 days, cultured in Matrigel for 12 days and then transitioned to 2% alginate for 53 days, and cultured in 2% alginate for 65 days had a similar profile of lung markers including lung marker NKX2.1, airway markers (P63, FOXJ1, MUC5AC, SCGB1A1) and alveolar markers (SFTPC, HOPX, T1alpha). All error bars represent SEM from $n = 3$ for each group. Data presented as fold change from hPSC control. Scale bars apply to all images with the subfigure unless otherwise noted. HLOs, human lung organoids; hPSC, human pluripotent stem cell. Color images are available online.

culture (Fig. 1A). Although the alginate restrained mesenchymal outgrowth, the overall size of the HLO increased over time (Fig. 1A).

We next measured gene expression of lung epithelial marker NKX2.1, airway cell-type makers including P63 (basal cell), FOXJ1 (ciliated cell), MUC5AC (goblet cell), SCGB1A1 (club cell), and alveolar cell markers including SFTPC (type II cell) and HOPX and T1alpha (type I cell). No significant differences were observed in gene expression among the HLOs grown in Matrigel alone (65 days), HLOs initially grown in Matrigel (12 days) then transitioned to 2% alginate (53 days), and HLOs grown in 2% alginate the entire time (65 days; Fig. 1B). The HLOs possess similar lung marker gene expression whether cultured in Matrigel or alginate, suggesting the cell-type make-up of the epithelium in the organoid did not change based on the substrate the HLOs were cultured in.

The HLOs grown in 2% alginate had epithelial structures growing outward from the body of the organoid observed as early as day 30 in culture (Figs. 1A and 2A). In the native lung, the airway epithelium is coated with multiciliated cells that make up the majority of the lung airway epithelium and help coat the epithelium with mucins and remove debris.[30,31] HLOs grown in 2% alginate had multiciliated cells labeled by acetylated tubulin (ACTTUB) at day 49 in culture. As early as day 66 of culturing HLOs in alginate, beating ciliated cells were readily observed (Supplementary Video S1). The 3D image reconstructions of the epithelial structures revealed ACTTUB$^+$ ciliated cells with the apical surface of the cells facing outward toward the surrounding substrate, whereas the P63$^+$ basal-like cells, which are the airway stem cell population in the native airway,[32] were located within the structures (i.e., closer to the body of the organoid) (Fig. 2C). For HLOs cultured in Matrigel, ACTTUB labeling at the apical surface of cells was observed by day 65, yet no cilia developed (Fig. 2B), and multiciliated cells labeled by ACTTUB appeared at day 80 in culture within the airway-like structures that are lined with P63$^+$ basal cells (Fig. 2B). Taken together, HLOs cultured in 2% alginate possess beating ciliated cells that appear as early as day 49 in culture.

Matrigel supplemented alginate improved the health of HLOs

Organoid health at day 5 in culture for HLOs grown in 2% alginate was 35%, much lower than that of HLOs grown in Matrigel (Fig. 3A, B). We hypothesized that the alginate physical properties may influence organoid health and investigated the culture of organoids in 1% alginate.

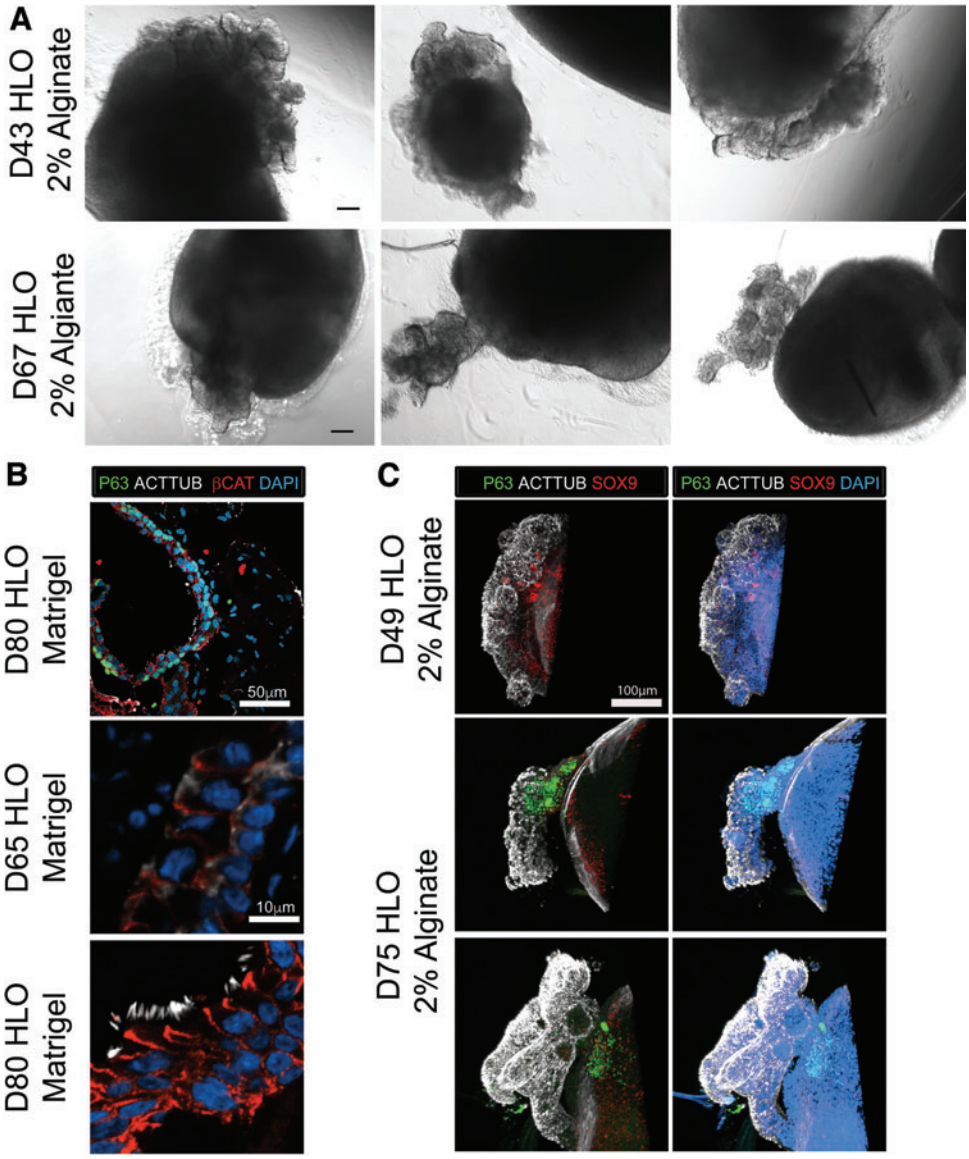

FIG. 2. HLOs grown in alginate express airway epithelial makers. **(A)** Epithelial structures were observed as early as 43 days in culture and were still observed at day 67. Scale bar represents 200 μm. **(B)** HLOs cultured in Matrigel have epithelial structures labeled by β-Catenin (*red*) that are lined with $P63^+$ basal cells (*green*) along the basal lamina with few multiciliated cells labeled by acetylated tubulin (ACTTUB, *white*). At day 65 (*middle panel*), the HLOs only have ACTTUB staining toward the apical side of the epithelial structures but no visible cilia. At day 80, HLOs have few multiciliated cells where the cilia are labeled with ACTTUB (*white*). **(C)** HLOs cultured in 2% alginate for 49 days and 75 days have $ACTTUB^+$ (*white*) multiciliated cells coating the epithelial structures. The $P63^+$ (*green*) cells labeling the basal cells were tucked in toward the HLO. Epithelial progenitor marker and proximal mesenchymal marker SOX9 (*red*) was scattered in the epithelial structures and the body of the HLOs. Scale bar is the same for all panels in the subfigure. Color images are available online.

No morphological differences were observed between the 1% and 2% alginate (Fig. 3A). We next investigated augmenting the physical properties with the biochemical cues available in Matrigel, which is an animal product that contains undefined levels of growth factors and biological cues. Matrigel was added to 2% alginate at ratios of Matrigel:2% alginate of 1:1 and 1:7. The 1:1 ratio produced organoids with similar morphology to 100% Matrigel, in which the mesenchyme grew from the body of the organoid at day 60 in culture (Fig. 3A). The 1:7 ratio had a significantly increased number of healthy organoids, with 68% of HLOs appearing healthy, and these HLOs had the same morphology as HLOs grown in 2% alginate (Fig. 3A, B). The percentage of healthy organoids per well was defined as the number of HLOs containing a clear epithelium surrounded by mesenchyme, whereas unhealthy or dead organoids were defined as having no observable epithelium and surrounded by dead or dying cells and cellular debris. As before, HLOs grown in Matrigel, 2% alginate, and ratios of 1:1 and 1:7 of Matrigel and 2% alginate had similar gene expression of lung markers (Fig. 3C).

HLOs grown in 1:7 ratio of Matrigel:2% alginate had the same epithelial structures observed in the alginate alone, with the outside of the epithelium coated in multiciliated cells labeled by ACTTUB and $P63^+$ basal cells nestled within the epithelium (Fig. 3D). In addition to the architecture, we observed $MUC5AC^+$ goblet-like cells (Fig. 3E). This cell type was not observed by protein staining in the HLOs grown in Matrigel although gene expression was detected in Matrigel-cultured HLOs.[7] Collectively, although the gene expression was not significantly different between ciliated cell marker FOXJ1 and goblet cell marker MUC5AC between Matrigel and alginate-grown HLOs, the morphology, epithelial structure, and protein expression were significantly different between HLOs grown in alginate versus 100% Matrigel.

IPF organoid model

The HLOs provided a unique opportunity to study diseases that affect the lung epithelium and mesenchyme such as IPF. IPF is a chronic, fatal disease with no current

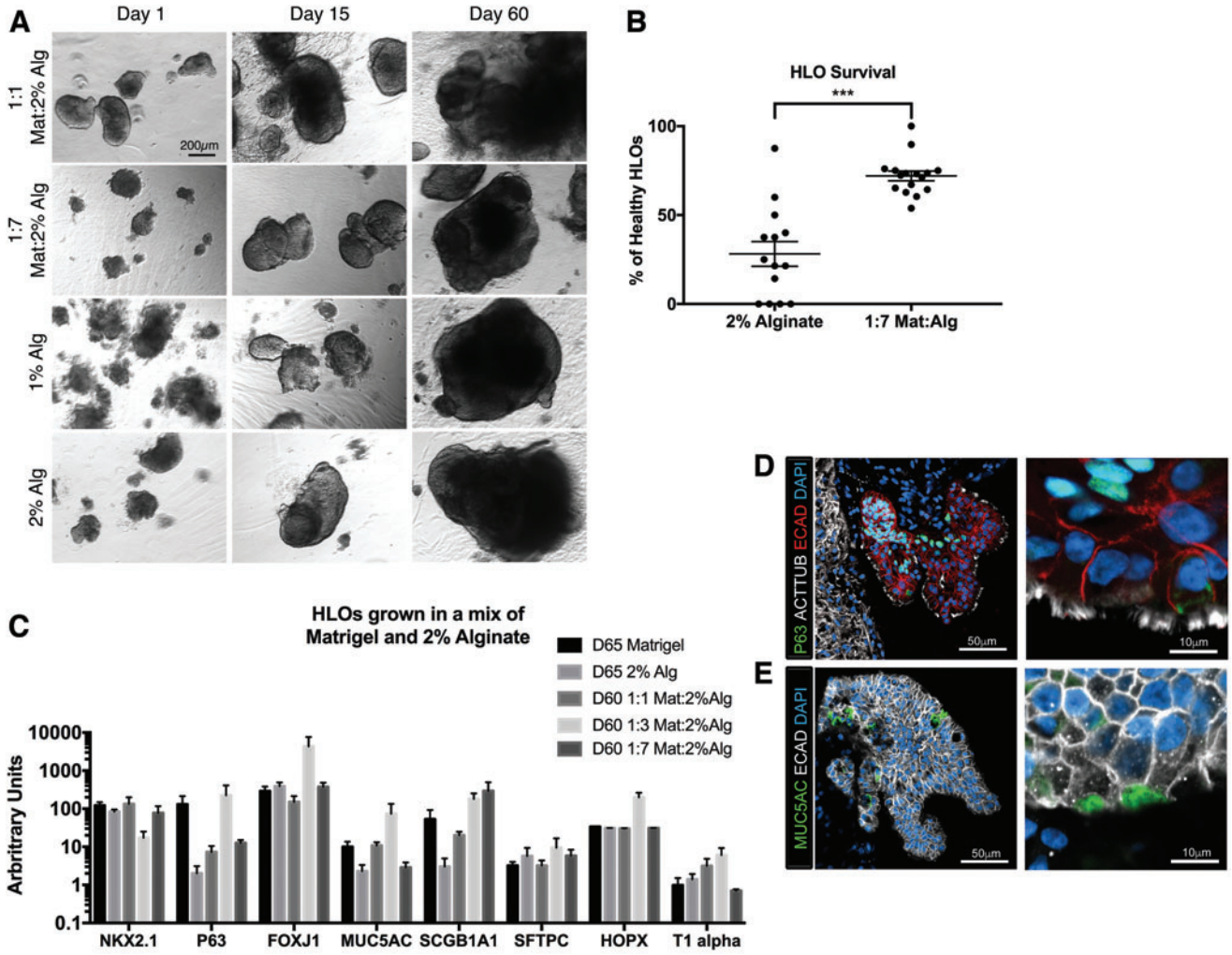

FIG. 3. Healthy HLOs increased when matrix was added to the alginate. **(A)** Wholemount images of HLOs cultured in 1:1 Matrigel:2% alginate, 1:7 Matrigel:2% alginate, 1% alginate, and 2% alginate over 60 days. Scale bar applies to all images. **(B)** HLOs cultured in 1:7 Matrigel:2% alginate had significantly higher initial rate of healthy organoids (72.1% ± 2.7%, $n = 16$ alginate droplets) compared with 2% alginate (28.2% ± 6.5%, $n = 14$ alginate droplets). HLOs were quantified after 5 days in the alginate droplet. Error bars represent SEM. **(C)** HLOs grown in 100% Matrigel, 2% alginate. 1:1 Matrigel:2% alginate, and 1:7 Matrigel:2% alginate for 60–65 days had similar expression of lung marker NKX2.1, airway markers (P63, FOXJ1, MUC5AC, SCGB1A1), and alveolar markers (SFTPC, HOPX, T1alpha). All error bars represent SEM from $n = 3$ for each group. Data presented as fold change from hPSC control. **(D)** 1:7 Matrigel:2% alginate HLOs cultured for 60 days had multiciliated cells labeled by ACTTUB (*white*) covering the epithelial structures labeled by ECAD (*red*). The $P63^{+}$ (*green*) basal cells labeled were on the basal side of the epithelium, forming a pseudostratified epithelium. **(E)** 1:7 Matrigel:2% alginate HLOs cultured for 60 days had $MUC5AC^{+}$ (*green*) mucus producing goblet cells within the epithelium labeled by ECAD (*white*). Color images are available online.

therapies that halt or revert the effects of the disease. The current models of IPF, which include cell lines, primary tissue sections, and mouse models, have furthered our understanding of IPF, but have thus far failed to lead to significant improvement in therapeutic options to treat IPF.[33,34] IPF deteriorates the alveolar epithelium and causes an overgrowth of mesenchymal myofibroblasts.[34] The HLOs we describe here comprised alveolar epithelial cell types and mesenchyme including fibroblasts and myofibroblasts,[7,24] providing a unique opportunity to study fibrosis and the interaction of the epithelium and mesenchyme. During IPF, myofibroblasts become activated and begin to increase in number and express smooth muscle actin (SMA).[34,35]

We first treated HLOs in 100% Matrigel and 1:7 Matrigel:2% alginate (hereafter termed the alginate condition) with 100 ng/mL of TGFβ for 7 days. In this initial study, no morphological differences were observed in treated and untreated HLOs grown in Matrigel (Fig. 4A). Furthermore, no difference in the gene expression of SMA was detected, and expression of the mesenchymal marker vimentin (VIM) was slightly reduced in the treated Matrigel HLO group compared with the nontreated Matrigel HLO group (Fig. 4B). For the HLOs grown in alginate, TGFβ stimulation resulted in significantly increased SMA gene expression and moderately increased VIM expression (Fig. 4B). Subsequent studies focused on HLOs grown in

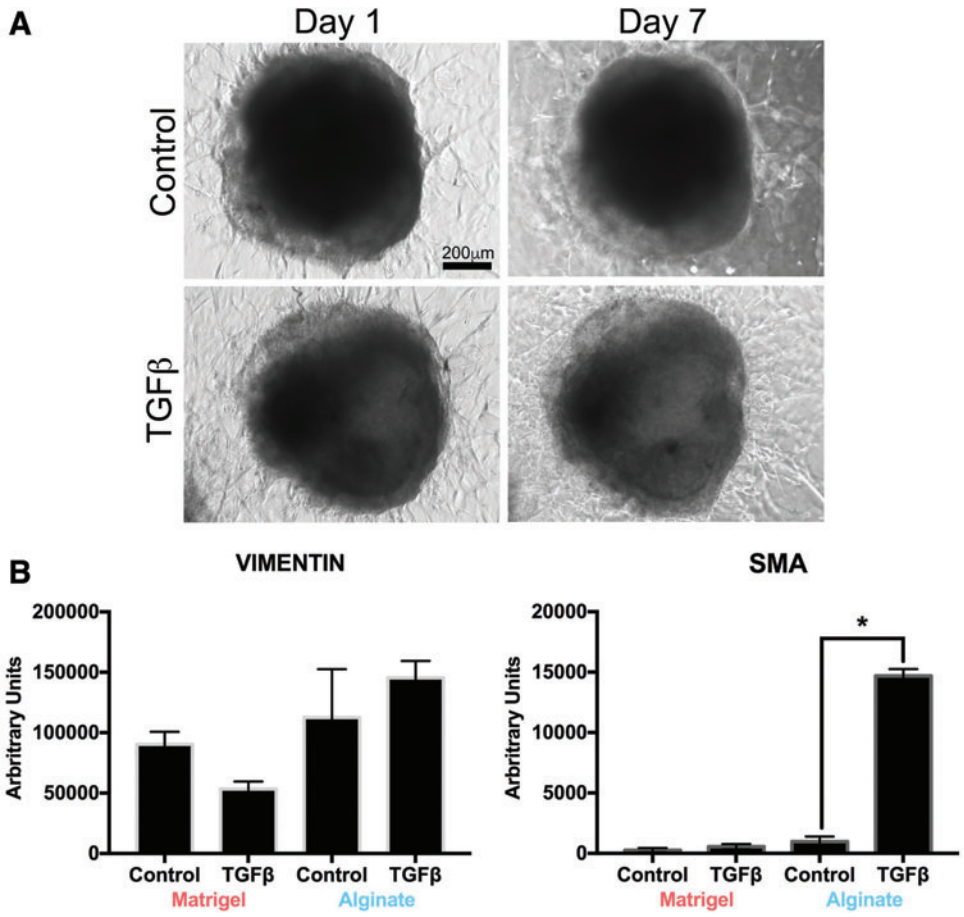

FIG. 4. HLOs cultured in Matrigel did not have a fibrotic phenotype when treated with TGFβ. **(A)** Wholemount images of HLOs cultured for 60 days treated with TGFβ for 7 days had the same mesenchymal outgrowth as the untreated group. Scale bar applies to all images. **(B)** HLOs in Matrigel cultured for 55 days and then treated with TGFβ for 28 days had a slight decrease in expression of the mesenchymal marker vimentin and no significant increase in myofibroblast marker SMA. HLOs cultured in 1:7 Matrigel:2% alginate (labeled Alginate) had a slight increase in vimentin transcript and significant increase in SMA transcript. All error bars represent SEM from $n = 3$ for each group. Data presented as fold change from hPSC control. SMA, smooth muscle actin; TGFβ, transforming growth factor β. Color images are available online.

alginate to model fibrosis. Of importance, because alginate cultured HLOs do not need to be continuously split every 2 weeks, this allowed for extended studies.

We next investigated the impact of sustained TGFβ stimulation on the morphology and gene expression in the HLOs. TGFβ stimulation was initiated on day 55 in HLOs grown in 1:7 Matrigel/alginate and was sustained for 4 weeks where media was changed every 3 days with fresh TGFβ (end of study: day 83 of HLOs; Fig. 5A). The 4-week TGFβ-treated HLOs had drastic changes in their morphology, with mesenchymal projections protruding from the body of the organoid compared with the control (Fig. 5B). We also observed an increased number of SMA^+ cells compared with the control by immunofluorescence (IF), which correlated with a significantly higher SMA gene expression compared with the untreated HLOs by qRT-PCR (Fig. 5C, D).[34]

In addition to an increase in SMA^+ cells, the TGFβ-stimulated HLOs had a decrease in $SFTPC^+$ cells and a significant reduction in the gene expression of SFTPC, observed by IF and qRT-PCR, respectively (Fig. 5E, F). Decreased alveolar type II cells, expressing SFTPC, mirrors the phenotype observed in IPF patients.[34,36] We investigated the expression of key IPF markers by qRT-PCR and observed significant increases in gene expression for COL1A1 and COL3A1 in the TGFβ-treated HLOs relative to untreated HLOs, whereas the lung marker NKX2.1 and mesenchymal marker VIM were not significantly different between treatment and no treatment HLO groups (Fig. 5G–J).

We further confirmed these findings by comparing TGFβ-treated HLOs and untreated HLOs using scRNAseq. After initial clustering of all HLO cells, we identified nine clusters represented by both control and TGFβ-treated HLOs (Fig. 6A and Supplementary Fig. S1A, B). We first visualized the mesenchymal and epithelial cells by high expression of canonical markers for each of these cell types, through which we identified one clear mesenchymal cluster (Cluster 8) and two clusters that contained most of the epithelial cells (Clusters 1 and 6) (Fig. 6B). These clusters were identified generally as epithelial cells by high expression of keratins and calcium binding proteins (Fig. S1B). Upon closer evaluation of highly expressed genes in each cluster, we identified cell clusters represented primarily by ciliated cells, basal cells, lung-like mesenchyme, neuronal cells, and some nonlung cell lineages (Supplementary Fig. S1C, D).

We decided to focus the analysis on the mesenchymal cells as they appeared to be a clear and independent cell cluster and are relevant to IPF. After reclustering of the mesenchymal cells (Fig. 6C), we identified chondrocytes, myofibroblasts, and smooth muscle cells in TGFβ-treated HLOs and untreated HLOs as well as a population of mesenchyme present only in TGFβ-treated HLOs, hereafter termed IPF-induced mesenchyme (Fig. 6C, D). New populations of mesenchymal cells in IPF patients have been described before.[37] The IPF-induced mesenchyme in the TGFβ-treated HLOs express high levels of COL2A1 and COL1A2 (Fig. 6E), which are known markers of IPF-

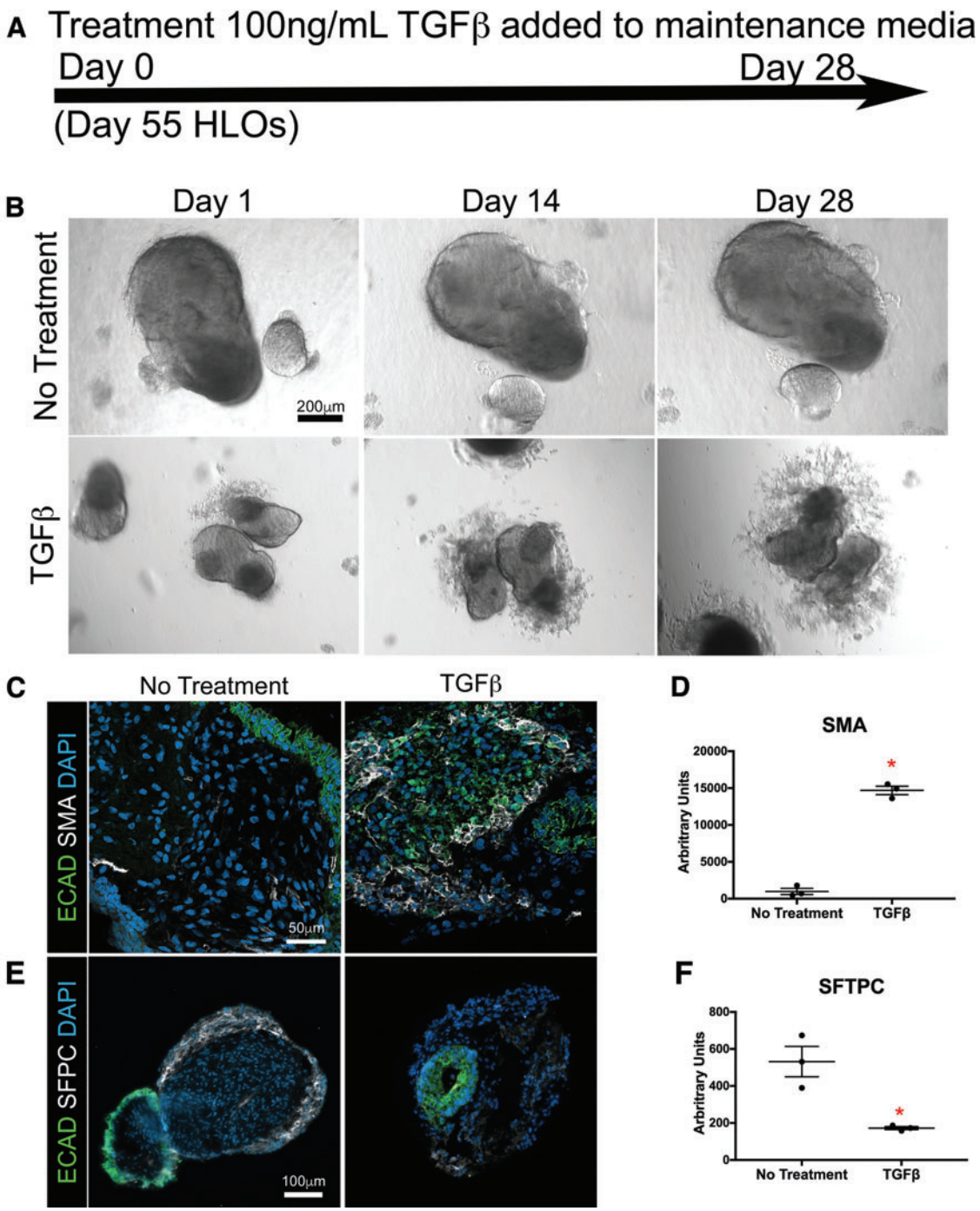

FIG. 5. HLOs grown in alginate gained a fibrotic phenotype when treated with TGFβ. **(A)** Timeline of TGFβ treatment. Treatment started with HLOs cultured for 55 days, then 100 ng/mL of TGFβ was added for 4 weeks. HLOs were cultured for a total of 83 days. **(B)** HLOs treated with TGFβ had mesenchymal outgrowths compared with the untreated group. **(C)** There was an increase of SMA^+ (*white*) cells, which label myofibroblasts, in the TGFβ treated group compared with the untreated group. Epithelium was labeled by ECAD (*green*). **(D)** There was a significant increase of SMA transcript in the TGFβ-treated group compared with the untreated group. **(E)** The TGFβ treated group had fewer $SFTPC^+$ (*white*) cells compared with the untreated group. SFTPC labels type II alveolar cells and alveolar progenitors. Epithelium was labeled by ECAD (*green*). **(F)** There was a significant decrease of SFTPC transcript compared with the untreated group. **(G, H)** COL1A1 and COL3A1 mRNA expression were significantly higher in the TGFβ-treated group compared with the untreated group. **(I, J)** TGFβ-treated and untreated groups had similar mRNA expression of early lung marker NKX2.1 and mesenchymal marker vimentin. All error bars represent SEM from $n = 3$ for each group. Data are presented as fold change from hPSC control. Scale bars in **(B)**, **(C)**, and **(E)** apply to all parts of the subimage. $*p < 0.05$. Color images are available online.

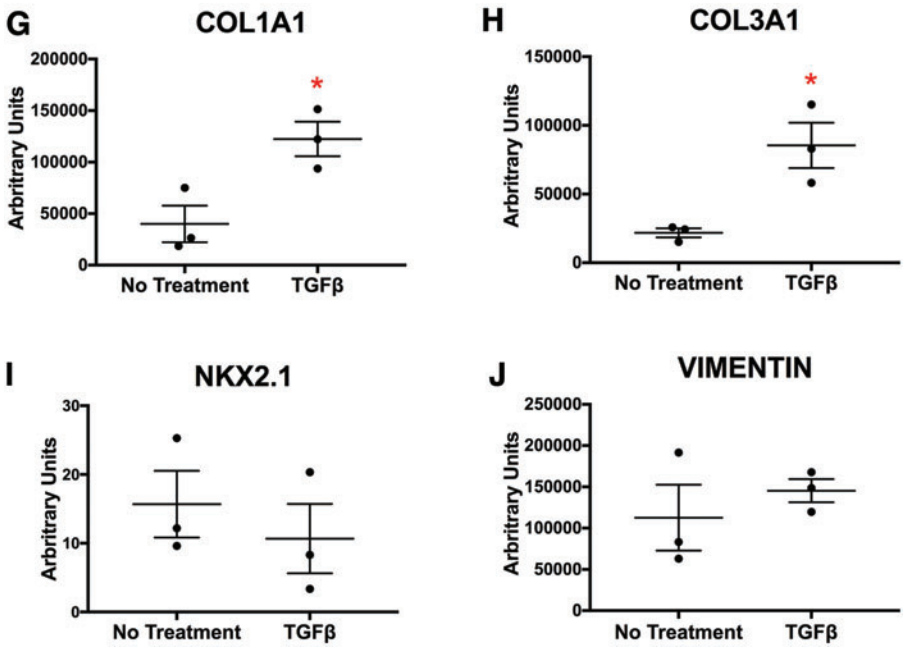

FIG. 5. (Continued).

induced mesenchyme in humans *in vivo*.[37] Chondrocytes, myofibroblasts, and smooth muscle cells were identified by determining high expression of canonical markers for each of the identified cell types (Fig. 6E). A more complete list of differentially expressed genes is given in Supplementary Tables S1 and S2.

Finally, we investigated the expression of key IPF markers in our scRNAseq data.[34,38] Increases in gene expression were observed for COL1A1 and COL3A1 in the TGFβ-treated HLOs relative to untreated HLOs; however, we saw that the upregulation of these markers is almost entirely from the IPF-induced mesenchyme rather than an increase in expression from myofibroblasts, smooth muscle cells, or chondrocytes (Fig. 6F). In addition, other markers previously described to be up- or downregulated during IPF[39] were up- and downregulated in the TGFβ-treated HLOs, respectively. These include upregulation of SM22 and downregulation of FBLN1 (Fig. 6F). In addition to expressing known IPF markers, the IPF-induced mesenchyme appears to have a unique expression profile, with multiple genes enriched in these cells compared with the other mesenchymal cell types (Fig. 6G). Of importance, Cluster 2 within the mesenchymal cluster consisted solely of TGFβ-treated cells and upregulated gene ontology pathways associated with ECM and organization (Fig. 6H), consistent with the organoid morphology observed in Figure 5.

Discussion

Emerging advancements with organoids have improved culture systems that support the differentiation and assembly of multiple cell types into normal organ structures, which can be used to model complex diseases. Although Matrigel has been a popular choice for 3D culture, synthetic and natural materials have also been used; for example, intestinal organoids have recently been cultured in polyethylene glycol and alginate hydrogels.[12–15] In particular, intestinal organoids derived from hPSCs had enhanced organization when grown in the nondegradable, natural biomaterial alginate.[13] We applied an alginate-based hydrogel system to HLOs, which supported the formation of the HLO epithelium and mesenchyme, including the development of more diverse cell types within the airway epithelium compared with HLOs in Matrigel.

HLOs cultured in 2% alginate possessed epithelial structures that resembled native airway epithelium including beating multiciliated cells with scattered mucus producing goblet cells and $P63^+$ basal cells along the basal lamina toward the body of the organoid. This cell differentiation occurred as early as day 50 in culture compared with day 80 in Matrigel-cultured HLOs, where only a few ciliated cells were observed with no goblet cells present. Further investigation is needed determine the causation of the inside-out morphology of the derived airway epithelium by studying both the force and ECM deposition in the alginate. Because similar inside-out morphology occurred with the Matrigel supplemented alginate, we believe this may be caused by force and interaction with the alginate. The restrained growth of mesenchyme in alginate allowed for the analysis of TGFβ treatment on the development of fibrosis, where myofibroblasts expanded within the HLOs, markers of alveolar type II cells were reduced, IPF-induced mesenchymal and ECM markers and cell types increased, and mesenchymal protrusions grew from the body of the organoid.

Although improved airway epithelium was observed in alginate alone, we observed enhanced initial healthy of the HLOs when supplemented with just one-eighth Matrigel. The Matrigel likely helps with the initial health and growth of the HLOs until degraded as the Matrigel contributes soluble factors that may help the HLOs to deposit their own matrix and survive long term. The initial growth factors and proteins that help with the initial health of the HLOs still need to be determined. The Matrigel was not replaced

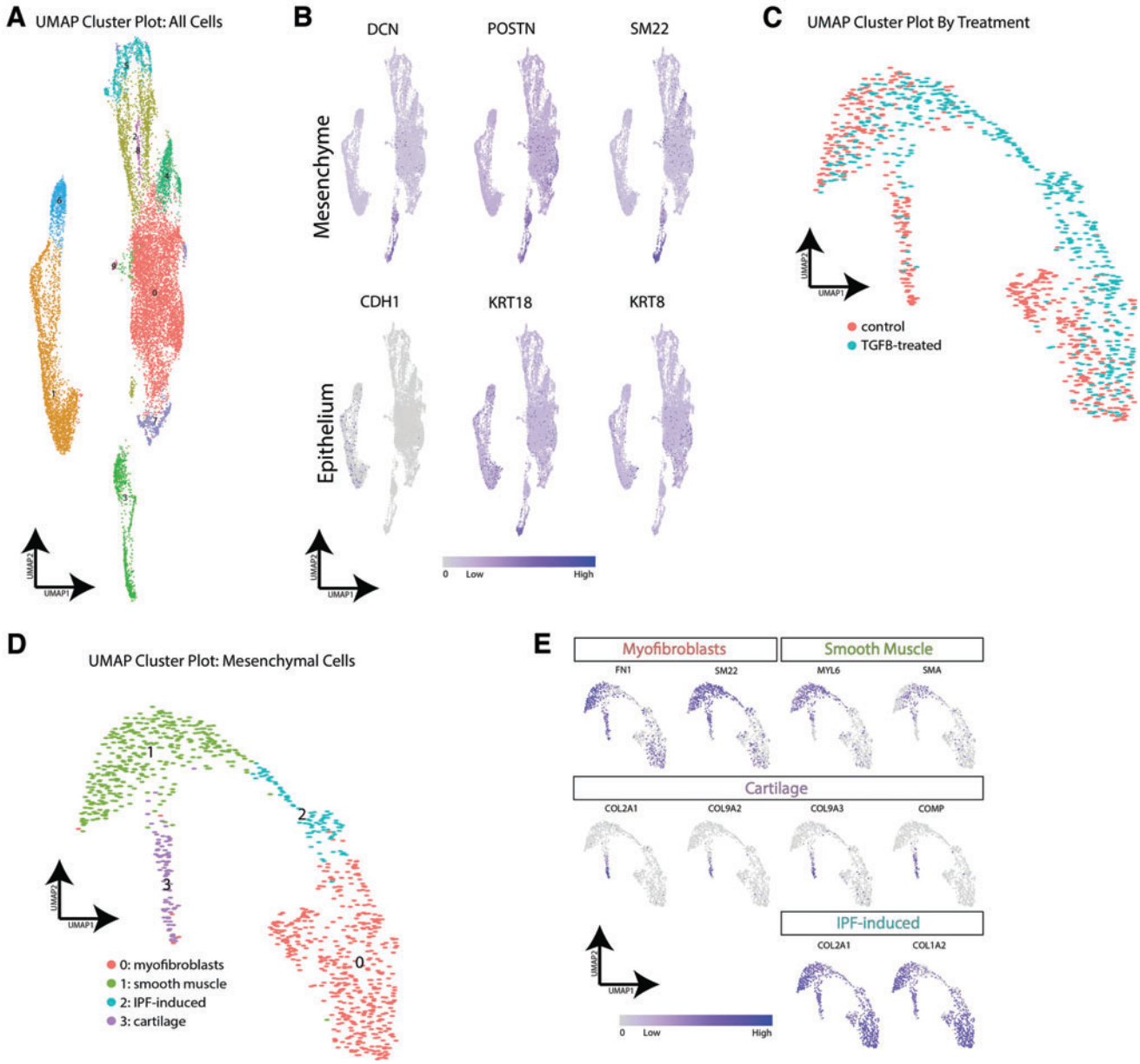

FIG. 6. scRNAseq analysis confirms a fibrotic phenotype in HLOs treated with TGFβ. **(A)** scRNAseq cluster plot from TGFβ-treated HLOs and control (untreated) HLOs. Each *dot* represents a single cell and cells are grouped based on transcriptional similarities. Nine cell clusters were identified. **(B)** Feature plots highlighting canonical mesenchymal markers (DCN, POSTN, SM22) and canonical epithelial markers (CDH1, KRT18, KRT8). Cluster 3 was identified as the mesenchymal cell cluster, whereas Clusters 1 and 6 appeared to contain the epithelial cells. **(C)** scRNAseq cluster plot from just the mesenchymal cells in TGFβ-treated HLOs and control HLOs. The cluster plot is colored by cells from TGFβ-treated HLOs or control HLOs. Clusters 0, 1, and 3 contain cells from control and TGFβ-treated HLOs, whereas Cluster 2 contains cells from only the TGFβ-treated HLOs. **(D)** scRNAseq cluster plot from just the mesenchymal cells in TGFβ-treated HLOs and control HLOs. Cell type labels are based on expression of canonical markers for each cell type identified or based on genes most highly enriched by cells in a cluster. **(E)** Feature plots showing expression of cell type markers used to identify clusters. Myofibroblast markers are enriched in Cluster 0, smooth muscle cell markers are enriched in Cluster 1, and chondrocyte markers are enriched in Cluster 3. COL2A1 and COL1A2 are highly expressed in the IPF-induced cell cluster (Cluster 2). **(F)** Violin plots identifying known IPF-induced genes that are up- or downregulated in TGFβ-treated HLOs. **(G)** Box plots showing six of the most highly enriched genes in the IPF-induced cell cluster (Cluster 2) compared with the other cell clusters. **(H)** Gene ontology pathways upregulated in marker genes from Cluster 2. IPF, idiopathic pulmonary fibrosis; scRNAseq, single cell RNA sequencing. Color images are available online.

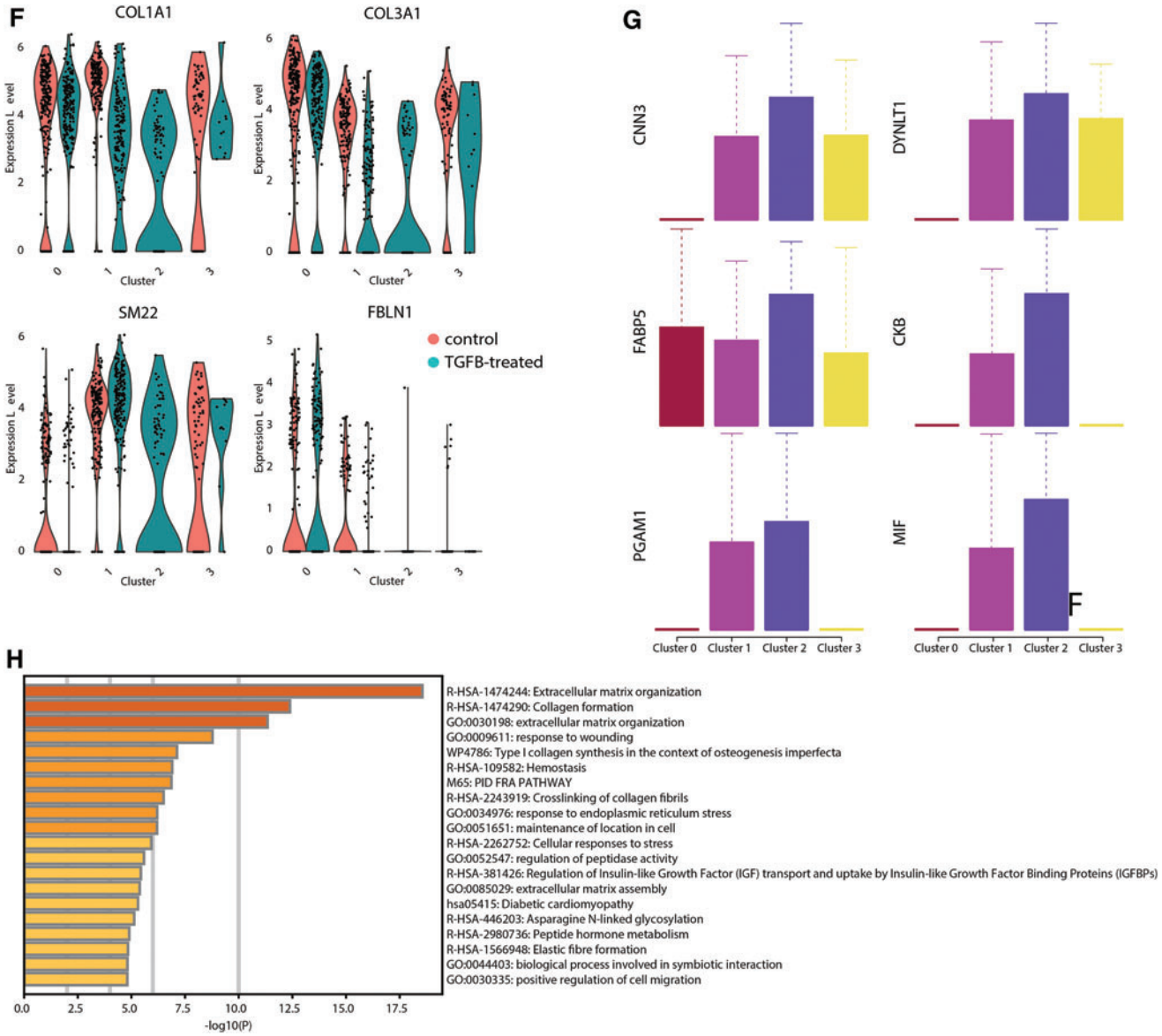

FIG. 6. (Continued).

during the 100+ days of culture. In comparison with other hPSCs lung organoid models, which are epithelial-only organoids that model airway epithelium in a cyst-like structure,[40] one of the main advantages of this HLO model is the combination of the lung epithelium and supporting mesenchyme, which enables investigating the interaction of epithelium and mesenchyme in a disease context. We hypothesize that in the 100+ day cultures where the supplemented Matrigel was not replaced, the alginate provides a 3D structure without inhibiting growth allowing the HLO matrix and mesenchyme to support the epithelial tissue. This hypothesis is further supported in which epithelial-only organoids can only be grown in alginate unless co-cultured with mesenchymal cells.[13] Further research is necessary to determine the potential differences of the lung organoid mesenchyme in alginate compared with Matrigel. Relative to Matrigel-grown HLOs, where ciliated cells face the inside of the organoid and basal cells line the outside surface of the organoid, alginate grown HLOs were inside-out. Based on recent reports, this could be owing to the lack of ECM proteins in alginate, which help control polarity.[41]

We were able to develop an IPF HLO model with HLOs grown in alginate. IPF causes hypoplastic and a loss of alveolar cells, increased bronchiolization in the alveolar epithelium, fibrosis in the mesenchyme, and an overgrowth of ECM.[42] IPF is a disease of unknown origin that permanently damages the lungs and leads to >50,000 deaths per year in the United States (pulmonaryfibrosis.org). It is chronic, progressive, and fatal, and only two therapies exist that mildly slow but do not halt the progression of the disease in some patients.[33,34,42] Mouse models treated with Bleomycin are the primary system for studying IPF; however, recent findings suggest that structural, cellular, and functional differences exist between healthy mouse and human lungs, which make it difficult to model IPF in mice.[33] In addition, the mouse model reverts back to normal lung phenotype over time with no treatment,

which contradicts the progression of fibrosis in the human disease.[33,43] A small amount of 2D and 3D human-specific *in vitro* models of IPF exist; however, many are limited in source and none effectively model epithelial–mesenchymal or cell–matrix interactions.[43] Thus, improved IPF models are needed. TGFβ stimulation of HLOs grown in alginate provided a combination of epithelium, controlled growth of the mesenchyme, and HLO-supplied ECM that enables the modeling of IPF. In contrast, HLOs grown in 100% Matrigel did not exhibit markers of IPF most likely because of Matrigel already containing TGFβ that may be the catalyst of the mesenchyme outgrowth that needs to be trimmed every 2 weeks.

Using scRNAseq, we identified multiple epithelial and mesenchymal cell types in HLOs, including ciliated cells, basal cells, myofibroblasts, smooth muscle cells, and chondrocytes. Upon treatment with TGFβ, an IPF-induced mesenchymal population arose, which expressed a unique gene expression profile including markers shown to be expressed in IPF-induced mesenchymal cells in IPF patients.[37] HLOs treated with TGFβ also had an increase in IPF markers along with a decrease in the alveolar marker SFTPC, which correlates with the phenotype in IPF patients. A recent report indicated that *Pdgfra*$^{+}$ mesenchymal cells in mice proliferate and upregulate SM22 in the IPF diseased state and are therefore at least partially responsible for fibrosis in IPF.[35]

The IPF HLO model allows further study of the contribution and changes of these cells in a human-specific model as the fibrotic phenotype progresses in culture under TGFβ treatment. In contrast to the Bleomycin-treated mouse model, the HLO model can be used to study initiation and progression of fibrosis, whereas the mouse model for IPF has initiation of fibrosis but does not progress overtime.[33] In addition to using the IPF HLO model to study the origin and progression of the disease and changes in cell types and ECM composition, the model can be used to study signaling pathways that could be potential therapeutic targets for IPF, and it could provide a high-throughput platform for drug and therapy testing. Thus, the HLO IPF model may provide insight into how to treat the progression of the disease and what signaling pathways propagate the disease.

In this report, we have demonstrated enhanced airway cell differentiation when HLOs are cultured in the natural biomaterial alginate. We observed an increase in the number of multiciliated cells, the most prevalent cell type in the lung airway, mucus-producing goblet cells, and basal cells organized in a flipped pseudostratified epithelium similar to the native lung airway. This enhanced differentiation occurred as early as day 50 in culture compared with HLOs cultured in Matrigel for 80 days when only a few multiciliated cells and no goblet cells were observed. HLO initial health increased when a small portion of Matrigel was added to the alginate. The Matrigel likely degraded overtime, resulting in the same enhanced differentiation observed in the HLO alginate alone cultures. Finally, because the HLOs possess alveolar epithelial cells and the alginate controlled the growth of the supporting mesenchyme, the HLOs modeled aspects of IPF including gross fibrotic outgrowth, increased ECM gene expression, increased numbers of mesenchymal cells including a new cell population, and decreased numbers of alveolar epithelial cell types. Not only did the HLO cultures in alginate promote rapid and improved airway cell differentiation, the system allowed for a novel model for IPF that may provide new insights for this devastating disease.

Authors' Contributions

B.R.D., R.F.C.H., A.J.M., and S.H. performed the experiments. J.T.D. analyzed the sequencing data. B.R.D., L.D.S., and J.R.S. conceptualized the experiments. B.R.D., J.T.D., L.D.S., and J.R.S. wrote the article. All authors read and approved the article before publication.

Data Availability

Single cell sequencing data is accessible through the Gene Expression Omnibus (Accession No. GSE171331). Other data associated with this article are available upon request.

Disclosure Statement

No competing financial interests exist.

Funding Information

This research was funded by NIH grant 5R01AI155678 and R01DK121462 (L.D.S. and J.R.S.). J.T.D. is funded by NIH grant 5K01EB028877.

Supplementary Material

Supplementary Figure S1
Supplementary Table S1
Supplementary Table S2
Supplementary Video S1

References

1. Dedhia PH, Bertaux-Skeirik N, Zavros Y, et al. Organoid models of human gastrointestinal development and disease. Gastroenterology 2016;150(5):1098–1112; doi: 10.1053/j.gastro.2015.12.042
2. Fatehullah A, Tan SH, Barker N. Organoids as an in vitro model of human development and disease. Nat Cell Biol 2016;18(3):246–254; doi: 10.1038/ncb3312
3. Johnson JZ, Hockemeyer D. Human stem cell-based disease modeling: Prospects and challenges. Curr Opin Cell Biol 2015;37:84–90; doi: 10.1016/j.ceb.2015.10.007
4. Rookmaaker MB, Schutgens F, Verhaar MC, et al. Development and application of human adult stem or progenitor cell organoids. Nat Rev Nephrol 2015;11(9):546–554; doi: 10.1038/nrneph.2015.118
5. Dye BR, Miller AJ, Spence JR. How to grow a lung: Applying principles of developmental biology to generate lung lineages from human pluripotent stem cells. Curr Pathobiol Rep 2016;4(2):47–57; doi: 10.1007/s40139-016-0102-x
6. Jacob A, Vedaie M, Roberts DA, et al. Derivation of self-renewing lung alveolar epithelial type II cells from human pluripotent stem cells. Nat Protoc 2019;14(12):3303–3332; doi: 10.1038/s41596-019-0220-0
7. Dye BR, Hill DR, Ferguson MA, et al. In vitro generation of human pluripotent stem cell derived lung organoids. Elife 2015;4:e05098; doi: 10.7554/eLife.05098
8. Chen YW, Huang SX, de Carvalho AL, et al. A three-dimensional model of human lung development and disease from pluripotent stem cells. Nat Cell Biol 2017;19(5):542–549; doi: 10.1038/ncb3510

9. McCauley KB, Hawkins F, Serra M, et al. Efficient derivation of functional human airway epithelium from pluripotent stem cells via temporal regulation of Wnt signaling. Cell Stem Cell 2017;20(6):844–857; doi: 10.1016/j.stem.2017.03.001
10. Miller AJ, Spence JR. In vitro models to study human lung development, disease and homeostasis. Physiology 2017; 32(3):246–260; doi: 10.1152/physiol.00041.2016
11. Czerwinski M, Spence JR. Hacking the matrix. Cell Stem Cell 2017;20(1):9–10; doi: 10.1016/j.stem.2016.12.010
12. Gjorevski N, Sachs N, Manfrin A, et al. Designer matrices for intestinal stem cell and organoid culture. Nature 2016;539(7630):560–564; doi: 10.1038/nature20168
13. Capeling MM, Czerwinski M, Huang S, et al. Nonadhesive alginate hydrogels support growth of pluripotent stem cell-derived intestinal organoids. Stem Cell Reports 2019;12(2): 381–394; doi: 10.1016/j.stemcr.2018.12.001
14. Dye BR, Youngblood RL, Oakes RS, et al. Human lung organoids develop into adult airway-like structures directed by physico-chemical biomaterial properties. Biomaterials 2020;234:119757; doi: 10.1016/j.biomaterials.2020.119757
15. Cruz-Acuña R, Quirós M, Huang S, et al. PEG-4MAL hydrogels for human organoid generation, culture, and in vivo delivery. Nat Protoc 2018;13(9):2102–2119; doi: 10.1038/s41596-018-0036-3
16. Cruz-Acuña R, Quirós M, Farkas AE, et al. Synthetic hydrogels for human intestinal organoid generation and colonic wound repair. Nat Cell Biol 2017;19(11):1326–1335; doi: 10.1038/ncb3632
17. Caliari SR, Perepelyuk M, Cosgrove BD, et al. Stiffening hydrogels for investigating the dynamics of hepatic stellate cell mechanotransduction during myofibroblast activation. Sci Reports 2016;6(1):21387; doi: 10.1038/srep21387
18. Bidarra SJ, Barrias CC. 3D culture of mesenchymal stem cells in alginate hydrogels. Methods Mol Biol 2019;2002: 165–180; doi: 10.1007/7651_2018_185
19. Almqvist KF, Wang L, Wang J, et al. Culture of chondrocytes in alginate surrounded by fibrin gel: Characteristics of the cells over a period of eight weeks. Ann Rheum Dis 2001;60(8):781–790; doi: 10.1136/ard.60.8.781
20. Mhanna R, Kashyap A, Palazzolo G, et al. Chondrocyte culture in three dimensional alginate sulfate hydrogels promotes proliferation while maintaining expression of chondrogenic markers. Tissue Eng Part A 2014;20(9–10): 1454–1464; doi: 10.1089/ten.TEA.2013.0544
21. Andersen T, Auk-Emblem P, Dornish M. 3D cell culture in alginate hydrogels. Microarrays 2015;4(2):133–161; doi: 10.3390/microarrays4020133
22. Shea LD, Woodruff TK, Shikanov A. Bioengineering the ovarian follicle microenvironment. Annu Rev Biomed Eng 2014;16:29–52; doi: 10.1146/annurev-bioeng-071813-105131
23. Shikanov A, Xu M, Woodruff TK, et al. Interpenetrating fibrin–alginate matrices for in vitro ovarian follicle development. Biomaterials 2009;30(29):5476–5485; doi: 10.1016/j.biomaterials.2009.06.054
24. Miller AJ, Dye BR, Ferrer-Torres D, et al. Generation of lung organoids from human pluripotent stem cells in vitro. Nat Protoc 2019;14(2):518–540; doi: 10.1038/s41596-018-0104-8
25. Spence JR, Mayhew CN, Rankin SA, et al. Directed differentiation of human pluripotent stem cells into intestinal tissue in vitro. Nature 2011;470(7332):105–109; doi: 10.1038/nature09691
26. Rockich BE, Hrycaj SM, Shih HP, et al. Sox9 plays multiple roles in the lung epithelium during branching morphogenesis. Proc Natl Acad Sci 2013;110(47):E4456–E4464; doi: 10.1073/pnas.1311847110
27. Miller AJ, Yu Q, Czerwinski M, et al. In vitro and in vivo development of the human airway at single-cell resolution. Dev Cell 2020;53(1):117–128; doi: 10.1016/j.devcel.2020.01.033
28. Stuart T, Butler A, Hoffman P, et al. Comprehensive integration of single-cell data. Cell 2019;177(7):1888–1902; doi: 10.1016/j.cell.2019.05.031
29. Zhou Y, Zhou B, Pache L, et al. Metascape provides a biologist-oriented resource for the analysis of systems-level datasets. Nat Commun 2019;10(1):1523; doi: 10.1038/s41467-019-09234-6
30. Mercer RR, Russell ML, Roggli VL, et al. Cell number and distribution in human and rat airways. Am J Respir Cell Mol Biol 1994;10(6):613–624; doi: 10.1165/ajrcmb.10.6.8003339
31. Yaghi A, Dolovich MB. Airway epithelial cell cilia and obstructive lung disease. Cells 2016;5(4):40; doi: 10.3390/cells5040040
32. Rock JR, Randell SH, Hogan BL. Airway basal stem cells: A perspective on their roles in epithelial homeostasis and remodeling. Dis Model Mech 2010;3(9–10):545–556; doi: 10.1242/dmm.006031
33. Moeller A, Ask K, Warburton D, et al. The bleomycin animal model: A useful tool to investigate treatment options for idiopathic pulmonary fibrosis? Int J Biochem Cell Biol 2008;40(3):362–382; doi: 10.1016/j.biocel.2007.08.011
34. Martinez FJ, Chisholm A, Collard HR, et al. The diagnosis of idiopathic pulmonary fibrosis: Current and future approaches. Lancet Respir Med 2017;5(1):61–71; doi: 10.1016/S2213-2600(16)30325-3
35. Li R, Bernau K, Sandbo N, et al. Pdgfra marks a cellular lineage with distinct contributions to myofibroblasts in lung maturation and injury response. Elife 2018;7:e36865; doi: 10.7554/eLife.36865
36. Sisson TH, Mendez M, Choi K, et al. Targeted injury of type II alveolar epithelial cells induces pulmonary fibrosis. Am J Respir Crit Care Med 2010;181(3):254–263; doi: 10.1164/rccm.200810-1615OC
37. Tsukui T, Sun KH, Wetter JB, et al. Collagen-producing lung cell atlas identifies multiple subsets with distinct localization and relevance to fibrosis. Nat Commun 2020; 11(1):1–6; doi: 10.1038/s41467-020-15647-5
38. Lagares D, Ghassemi-Kakroodi P, Tremblay C, et al. ADAM10-mediated ephrin-B2 shedding promotes myofibroblast activation and organ fibrosis. Nat Med 2017; 23(12):1405–1415; doi: 10.1038/nm.4419
39. Reyfman PA, Walter JM, Joshi N, et al. Single-cell transcriptomic analysis of human lung provides insights into the pathobiology of pulmonary fibrosis. Am J Respir Crit Care Med 2019;199(12):1517–1536; doi: 10.1164/rccm.201712-2410OC
40. Konishi S, Gotoh S, Tateishi K, et al. Directed induction of functional multi-ciliated cells in proximal airway epithelial spheroids from human pluripotent stem cells. Stem Cell Reports 2016;6(1):18–25; doi: 10.1016/j.stemcr.2015.11.010

41. Co JY, Margalef-Català M, Li X, et al. Controlling epithelial polarity: A human enteroid model for host-pathogen interactions. Cell Rep 2019;26(9):2509–2520.e4; doi: 10.1016/j.celrep.2019.01.108
42. Evans KV, Lee JH. Alveolar wars: The rise of in vitro models to understand human lung alveolar maintenance, regeneration, and disease. Stem Cells Transl Med 2020; 9(8):867–881; doi: 10.1002/sctm.19-0433
43. Sundarakrishnan A, Chen Y, Black LD, et al. Engineered cell and tissue models of pulmonary fibrosis. Adv Drug Deliv Rev 2018;129:78–94; doi: 10.1016/j.addr.2017.12.013
44. Huang SX, Islam MN, O'Neill J, et al. Efficient generation of lung and airway epithelial cells from human pluripotent stem cells. Nat Biotechnol 2013;32(1):1–11; doi: 10.1038/nbt.2754

Address correspondence to:
Lonnie D. Shea, PhD
Department of Biomedical Engineering
Gastroenterology
University of Michigan
2200 Bonisteel Boulevard
Ann Arbor, MI 48109
USA

E-mail: ldshea@umich.edu

Received: March 8, 2022
Accepted: July 12, 2022
Online Publication Date: October 7, 2022